Current Applied Science and Technology e-ISSN: 2586-9396

Curr. Appl. Sci. Technol. 2026, Vol. 26 (No. 5), e0266980

Research article

Hydrogel Formulation from Sugar Palm Starch as an Application of Acne Patch

Tazkia Qonita Zahra[1], Noverra Mardhatillah Nizardo[1]* and Witta Kartika Restu[2]

[1]Department of Chemistry, Faculty of Mathematics and Natural Sciences, Universitas Indonesia, Depok, West Java, 16424, Indonesia
[2]Research Center for Chemistry, National Research, and Innovation Agency (BRIN), KST B.J Habibe, Serpong, South Tangerang, Banten, 15314, Indonesia

Received: 2 April 2025, Revised: 25 August 2025, Accepted: 2 September 2025, Published: 16 January 2026

Abstract

Acne patches are among the most popular acne treatments. These patches are used to protect lesions from contaminants and deliver active compounds to enhance healing. In this study, hydrogel-based acne patches from sugar palm starch reinforced with chitosan (FC1-TTO) or alginate (FA1-TTO) were developed. Citric acid was used as a crosslinking agent, glycerol as a plasticizer, and tea tree oil (TTO) as the anti-acne agent. The hydrogel patches, containing 50, 70, and 100 µg/mL of TTO, were characterized using the FTIR, SEM, UTM, and DSC techniques. Their performance was evaluated based on encapsulation efficiency, drug release, and antibacterial properties. Both types of hydrogels containing 100 µg/mL of TTO showed high antibacterial activity against *Cutibacterium acnes*, *Staphylococcus aureus*, and *Staphylococcus epidermidis*, with inhibition zones up to 15 mm. Encapsulation efficiencies reached 95.98±0.24% for the FC1-TTO and 95.49±0.35% for the FA1-TTO. The cumulative TTO release after 6 h was 64.14% for the FC1-TTO and 85.08% for the FA1-TTO, indicating sustained release in both cases. In conclusion, sugar palm starch-based hydrogels reinforced with chitosan or alginate and loaded with 100 µg/mL TTO demonstrated effective antibacterial activity, making them a promising option for acne treatment.

Keywords: acne patch; hydrogel; polymer; sugar palm starch

1. Introduction

Acne vulgaris is a prevalent dermatological condition characterized by the clogging of hair follicles with sebum and dead skin cells, leading to bacterial proliferation such as *Cutibacterium acnes*, *Staphylococcus aureus*, and *Staphylococcus epidermidis*. Although acne is not dangerous, it can affect self-confidence and cause physical discomfort (Beheshti-Mall et al., 2018; Nascimento et al., 2023). Various acne treatments have been

*Corresponding author: E-mail: noverra.mardhatillah@sci.ui.ac.id
https://doi.org/10.55003/cast.2026.266980
Copyright © 2026 by King Mongkut's Institute of Technology Ladkrabang, Thailand. This is an open access article under the CC BY-NC-ND license (http://creativecommons.org/licenses/by-nc-nd/4.0/).

developed from topical (cream, lotion, and patch) and oral medications to reduce acne and prevent scarring based on the severity (mild, moderate, and severe). Nowadays, acne patches have become a popular choice due to their convenience and effectiveness. These small, transparent, adhesive patches are easy to use and gentle on the skin. The moist environment created by acne patches accelerates tissue regeneration, reduces inflammation, and minimizes scarring while shielding lesions from external contaminants. The patches also contain active ingredients that inhibit bacterial growth and enhance healing (Qothrunnadaa & Hasanah, 2021). One type of patches, hydrogel-based patch, absorbs excess oil and acne exudate due to its swelling properties, which occur because it contains hydrophilic groups such as $-SO_3H$, -OH, $-NH_2$, -COOH, and $-CONH_2$, which have a strong affinity to attract and hold water (Parhi, 2017; Berradi et al., 2023).

Tea tree oil is a popular active ingredient in anti-acne treatments. It is an essential oil extracted from the plant *Melaleuca alternifolia*. It contains 14 active compounds, with terpinene-4-ol being the primary constituent. TTO exerts its antimicrobial effects by disrupting microbial cell membranes, denaturing proteins, and inducing leakage of intracellular components, ultimately impairing bacterial viability. However, the therapeutic efficacy of TTO is limited by its volatility and thermolability. To overcome these challenges, encapsulation of TTO within hydrogel-based delivery systems has been explored. Encapsulation not only stabilizes TTO but also enables controlled release, enhancing its bioavailability and sustaining its antimicrobial activity (Nascimento et al., 2023).

Several studies have investigated hydrogels for skin applications, not only for anti-acne therapy but also for enhancing wound healing. For instance, Hu et al. (2023) developed a hydrogel composed of carboxymethyl chitosan (CMCS) and genipin incorporating TTO for the treatment of wounds. This formulation produced a hydrogel with an encapsulation efficiency of over 80% and exhibited antibacterial activity against *S. aureus* of over 90%. Another study conducted by Bisht et al. (2022) described a hydrogel for acne treatment composed of carbopol 934 and polyethylene glycol (PEG 400), incorporating azelaic acid and TTO as active ingredients. This formulation produced a hydrogel with strong inhibitory activity against *S. aureus, S. epidermidis,* and *C. acnes*, with zones of inhibition measuring up to 18 mm in diameter. Next, Kuo et al. (2021) developed a hydrogel from gelatin and chitosan with the active ingredients Cortex *Phellodendron amurense* (PA) and *Centella asiatica* (CA) extracts. The hydrogel demonstrated antibacterial activity with zones of inhibition measuring up to 26 mm in diameter. Additionally, the well-developed porous structure of the patches helps retain moisture and absorb exudate when applied to open acne wounds.

Biopolymer-based hydrogels are often used as wound dressings due to their superior biocompatibility, biodegradability, and non-toxicity compared to synthetic ones (Reddy et al., 2015). These biopolymers include starch, chitosan, and alginate polysaccharides, which are abundant in Indonesia. Starch, composed of amylose and amylopectin, is sourced from various agricultural products, including sugar palm (*Arenga pinnata*) (Jumaidin et al., 2016). Sugar palm starch was selected over other starch sources due to its non-competitive nature with food sources (Sanyang et al., 2016). Sugar palm starch is derived from trees that are no longer productive in producing sap, making it a byproduct or a waste material (Adawiyah et al., 2013). Chitosan is composed of glucosamine and N-acetylglucosamine derived from chitin in crustacean shells (Aranaz et al., 2021). Alginate is composed of α-L-guluronic acid (G) and β-D-mannuronic acid (M) monomers, derived from the extraction of brown algae or *Phaeophyceae* (Tomić et al., 2023). Both chitosan and alginate are derived from marine resources.

This study synthesized a biopolymer-based hydrogel loaded with TTO as the active agent. The novelty of this research lies in the use of biopolymers such as sugar palm

starch reinforced with chitosan or alginate to encapsulate TTO. According to the literature review, research on this specific combination is currently very limited. Several tests were conducted to evaluate the quality of the hydrogel, including thickness measurement, swelling ratio, functional group analysis using Fourier transform infrared (FTIR) spectroscopy, tensile strength, and elongation at break analysis using a universal testing machine (UTM), morphology image analysis using a scanning electron microscope (SEM), thermal analysis using differential scanning calorimetry (DSC), encapsulation efficiency, *in vitro* drug release analysis, and antibacterial activity.

2. Materials and Methods

2.1 Microorganisms

Cutibacterium acnes (ATCC 6919), *Staphylococcus aureus* (ATCC 6538), and *Staphylococcus epidermidis* (ATCC 12228) cultured on Nutrient agar (Oxoid CM0003, United Kingdom) were used in this study.

2.2 Materials and chemicals

Sugar palm starch (*Arenga pinnata*) with an amylose content of 23.19% was obtained from local industries in Klaten, East Java, Indonesia. Alginate was obtained from local industries in Yogyakarta, Indonesia. Water-soluble chitosan, sourced from shrimp with a degree of deacetylation of 50-60%, was obtained through a research collaboration with Universitas Sumatera Utara. Citric acid monohydrate (CAS: 5949-29-1, Merck, Germany), tea tree oil (commercial, 100% *Melaleuca alternifolia* with a terpinen-4-ol content of 38.9% was obtained from Banaran Soap, Purwokerto, Central Java, Indonesia), glycerol (United States Pharmacopeia (USP) grade), sodium chloride (NaCl) (CAS: 7647-14-5, Merck, Germany), ethanol (technical grade 96%), vancomycin HCl (HJ Generik), phosphate-buffered saline (PBS) (pH 7.4; 1x; TL1101-0500, HIMEDIA, India) and millipore (Mili-Q-ultrapure 18.2 MΩ·cm 25°C) were used for analysis. Distilled water served as solvent was obtained from a water purification system. Commercial acne patches from three different brands available in Indonesia (Dr. Lucky, Derma Angel, and Breylee) were used for comparison.

2.3 Preliminary assay of TTO: Determination of minimum inhibitory concentration (MIC) of TTO

The minimum inhibitory concentration (MIC) of TTO against the *C. acnes*, *S. aureus*, and *S. epidermidis* bacteria was determined using the broth microdilution method in a 96-well microtiter plate. The concentration of TTO used in this study was carefully selected according to previous findings by Greay et al. (2010), who confirmed that TTO concentrations of ≤300 µg/mL (≤0.03%) were non-cytotoxic to human fibroblast cells (HF32), as determined by the MTT assay. To ensure safety while maintaining potential efficacy, we prepared serial two-fold dilutions (100-0.78 µg/mL) from a 100 mg/mL TTO stock solution, with all tested concentrations below the reported cytotoxic threshold. Each well was inoculated with bacterial suspensions adjusted to 10^6CFU/mL. and plates were incubated for 24 h at 37°C under aerobic conditions. The MIC was determined visually as the lowest concentration showing no visible bacterial growth.

2.4 Synthesize of hydrogel patches

The hydrogels were synthesized using the solvent casting technique, as described by Wilpiszewska et al. (2019) with some minor adjustments. Three types of hydrogels were prepared: sugar palm starch-chitosan-TTO hydrogel (FC1-TTO), sugar palm starch-alginate-TTO hydrogel (FA1-TTO), and sugar palm starch hydrogel without a reinforcing agent and TTO (F0). The synthesis process began by dispersing sugar palm starch as the main polymer in purified water and heating the mixture at 70°C under stirring until complete gelatinization had occurred. Citric acid as a crosslinking agent was then added to the sugar palm starch solution while stirring continued. Next, glycerol was subsequently added as a plasticizer, with incorporation of either alginate or chitosan as reinforcing agents, or with omission in the control formulation. Once a homogeneous solution was achieved, various concentrations of TTO were incorporated in situ into the polymer solution for drug loading.

The selected concentrations were based on MIC results obtained from a preliminary assay, with 50 µg/mL identified as the minimum inhibitory concentration (data are not shown). Furthermore, the final mixture was stirred for 30 min to ensure uniform distribution, poured into a silicone cast and left at room temperature to minimize air bubble entrapment, and subsequently dried in an oven at 60°C until a constant weight was achieved. After drying, the hydrogel patches were removed from the cast, washed three times with purified water, air-dried overnight, and stored in a desiccator before further characterization. The detailed composition and properties of the hydrogels are listed in Table 1.

Table 1. The formulation of the hydrogel patches

Code	Formulations					
	Sugar Palm Starch (g)	Citric Acid (g)	Glycerol (mL)	Chitosan (g)	Alginate (g)	Tea Tree Oil (µg/mL)
F0	0.60	0.10	1.00	-	-	-
FC1-TTO 1	0.60	0.10	1.00	0.20	-	50
FC1-TTO 2	0.60	0.10	1.00	0.20	-	70
FC1-TTO 3	0.60	0.10	1.00	0.20	-	100
FA1-TTO 1	0.60	0.10	1.00	-	0.20	50
FA1-TTO 2	0.60	0.10	1.00	-	0.20	70
FA1-TTO 3	0.60	0.10	1.00	-	0.20	100

2.5 Characterization of the hydrogel patches

2.5.1 Thickness measurements

The thickness of the hydrogel patch was measured using a digital thickness gauge (Syntek-TGH000125, China) with a range of 0.0-25.4 mm and a resolution of 0.001 mm. Measurements were taken at 5 random spots to determine the average thickness and standard deviation.

2.5.2 Swelling ratio

The prepared hydrogel was weighed in its dry state before being immersed in PBS solution to reach the swelling state. The hydrogels were placed in a beaker containing 10 mL of PBS pH 7.4 solution and were immersed at specific time intervals (1, 2, 3, 4, 5, and 6 h) at 37°C. After each interval, the hydrogels were removed, blotted dry, and reweighed. The swelling ratio of the hydrogels was then calculated using equation (1) as follows (Arpa et al., 2023).

$$\text{Swelling ratio (\%)} = \frac{W_t - W_0}{W_0} x\ 100 \quad (1)$$

The initial hydrogel dry weight is denoted as W_0, and the hydrogel weight after immersion in PBS solution at a specific time is denoted as W_t.

2.5.3 Functional group analysis

Functional group analysis of the TTO, hydrogels loaded with TTO (100 µg/mL) and hydrogels without TTO was performed using a Fourier transform infrared (FTIR) spectrometer (Bruker-Tensor II, Germany). The samples were placed in an attenuated total reflectance (ATR) sample holder, and each sample was scanned in the wavelength range of 4000-400 cm^{-1} for 45 s at a resolution of 4 cm^{-1}.

2.5.4 Morphology analysis

The morphology of hydrogels, with and without TTO, was examined using SEM (JEOL JSM-IT200, Japan). Samples were lyophilized in a vacuum for 24 h, then mounted on carbon-coated holders and coated with gold via sputtering for 2 min. Observations were made at 1000x magnification with a 5 kV acceleration voltage.

2.5.5 Thermal analysis

Thermal analysis was performed using DSC (NETZSCH-214, Germany). A 5 mg hydrogel sample was placed in a sealed aluminum container and scanned from 25-300°C at a heating rate of 10°C/min in a nitrogen gas environment flowing at 20 mL/min.

2.5.6 Mechanical analysis

Mechanical analysis was performed using a UTM (AG-X Plus 50kN-Shimadzu, Japan) with a 50 kN load cell to evaluate tensile strength and elongation at break following ASTM D882-02 (2002). Hydrogel samples were divided into five specimens and conditioned for 40 h at 23±2°C (73.4±3.6°F) and 50±10% relative humidity. The test used a crosshead speed of 10 mm/min and a grip distance of 10 mm.

2.5.7 Encapsulation efficiency

The encapsulation efficiency of TTO in sugar palm starch-chitosan and sugar palm starch-alginate hydrogels was assessed using a modified method from Zhang et al. (2017). First, the absorbance of a standard TTO solution was measured using a UV-visible spectrophotometer (Genesys 150-Thermo Scientific, USA) at the maximum wavelength.

The absorbance values were then plotted on a calibration curve using the equation y = a + bx.

To calculate the oil content in the hydrogel, the surface oil content (M1) was first determined by rinsing the hydrogel five times with 25 mL of 96% ethanol and measuring the absorbance of the filtrate using a UV-visible spectrophotometer. The total oil content (M2) was then measured by immersing the hydrogel in 25 mL of 96% ethanol, sonicating for 60 min, and measuring the absorbance of this filtrate. The absorbance values of M1 and M2 were used with the linearity curve equation to calculate the oil content and determine the percentage of encapsulation efficiency. The percentage of encapsulation efficiency was then calculated using equation (2) below.

$$\text{Encapsulation efficiency (\%)} = \frac{M_2 - M_1}{M_2} x\ 100 \quad (2)$$

2.5.8 *In vitro* TTO release

The *in vitro* release testing of TTO was conducted by placing the hydrogel into a beaker containing 25 mL of PBS solution at pH 7.4, and maintaining at the temperature of 37°C. The mixture was stirred using a mechanical stirrer for 10 min. At specified time intervals of 1, 2, 3, 4, 5, and 6 h, aliquots of 1 mL were taken, and their absorbance was measured using a UV-visible spectrophotometer (Genesys 150-Thermo Scientific, USA) at the maximum wavelength. The concentration of TTO release was calculated by using the formula of absorbance against concentration. The percentage of encapsulation efficiency was then calculated using equation (3) below.

$$\textit{In vitro}\ \text{TTO release rate (\%)} = \frac{the\ amount\ of\ release\ TTO}{the\ amount\ of\ TTO\ in\ hydrogel\ patch} x\ 100 \quad (3)$$

2.5.9 Antibacterial activity assay of hydrogel patches

The antibacterial activity of hydrogel patches loaded with TTO against *C. acnes*, *S. aureus*, and *S. epidermidis* was tested using an agar diffusion method. Bacterial suspensions were prepared by diluting cultures in a sterile 0.90% (w/v) NaCl solution to a final concentration of 10^6 CFU/mL and adjusting the turbidity to match the 0.5 McFarland standard. Subsequently, 100 µL of each bacterial suspension was evenly spread onto a sterile nutrient agar plate. Hydrogel samples containing varying concentrations of TTO were placed on the surface of each inoculated nutrient agar plate, with tests conducted in triplicate. A sterile Whatman filter paper disk (6 mm) loaded with 10 µL of vancomycin (500 µg/mL) was used as a positive control, and a hydrogel without TTO (F0) was used as a negative control. The plates were incubated for 24 h at 37°C. After incubation, the inhibition zones around each hydrogel sample were observed as clear zones and measured using a ruler.

2.5.10 Stability test of hydrogel patches

Samples of hydrogel patches were kept at the three temperature conditions of 5±2°C (refrigerated), 25± 2°C (room temperature), and 40±2°C (accelerated condition) for a period of 7 days. During the storage period, the patches were observed and evaluated for changes in physical appearance (specifically color changes) and weight to assess their short-term stability under various temperature conditions.

2.6 Statistical analysis

Statistical analyses were performed for all quantitative data and were presented as the mean and standard deviation. An independent t-test was used for comparisons between two groups, while one-way analysis of variance (ANOVA) was applied for comparisons among three or more groups. A p-value < 0.05 was considered statistically significant.

3. Results and Discussion

3.1 Appearance and thickness of the hydrogel patch

The obtained hydrogels are presented in Figure 1. The hydrogel made from sugar palm starch-chitosan (FC1-TTO) appeared translucent white because the chitosan used came from the deacetylation of white shrimp shells. In contrast, the hydrogel from sugar palm starch-alginate (FA1-TTO) was yellowish-brown because the alginate used came from the extraction of brown algae. Among the two synthesized sugar palm starch-based hydrogels, the one that visually resembled commercially available acne patches the most was the FC1-TTO, as depicted in Figure 2, which shows the synthesized and commercial hydrogel acne patches applied to the back of a human hand, simulating acne patch application on the skin.

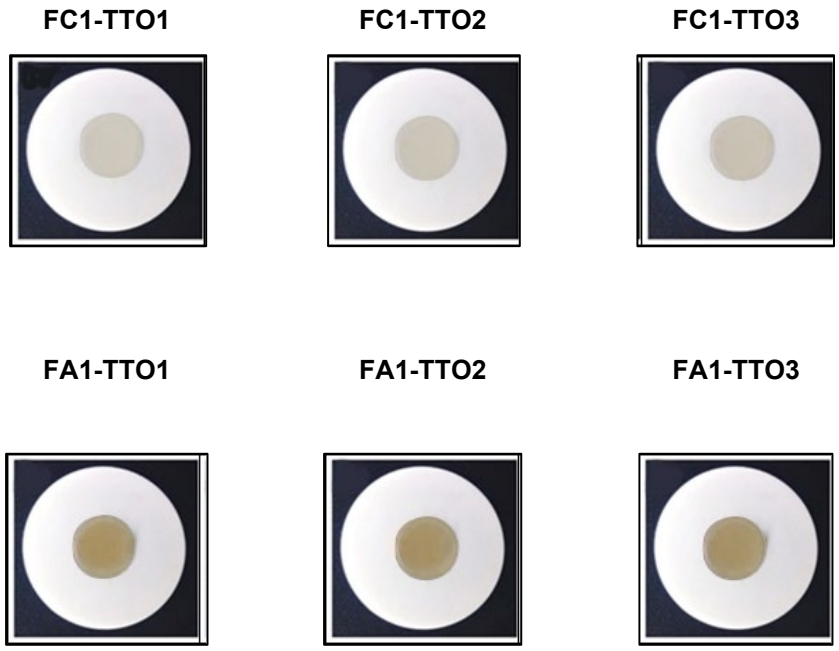

Figure 1. Appearance of TTO-loaded hydrogel patches

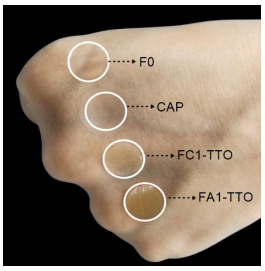

Figure 2. Visualization of acne patches applied to the back of a human hand; sugar palm starch hydrogel without a reinforcing agent and TTO (F0), commercial acne patch (CAP), sugar palm starch-chitosan-TTO hydrogel (FC1-TTO), and sugar palm starch-alginate-TTO hydrogel (FA1-TTO).

The measurement results for the thickness of the sugar palm starch-based hydrogels are presented in Table 2. Although the average thickness of FA1-TTO hydrogels appeared slightly higher than that of FC1-TTO hydrogels, the difference was not statistically significant ($p>0.05$), indicating that the type of reinforcing agent did not have a significant effect on the final thickness of the hydrogel. Similarly, the incorporation of TTO at different concentrations also did not significantly affect the thickness ($p>0.05$), according to one-way ANOVA statistical analysis.

Furthermore, the coefficient of variation (%CV) for thickness values ranged from 0.00% to 2.21%, demonstrating minimal variability and high consistency across hydrogel formulation batches. For comparison, the thickness of three commercially available acne patches (CAP) in the Indonesian market was also measured. The results showed that the thickness of the hydrogels acne patches developed in this study (0.21-0.29 mm) fell within the range observed for CAP (0.10-0.30 mm). These findings align with values reported in previous studies, which range from 0.148-0.238 (Arpa et al., 2023) to 0.34-0.52 mm (Simões et al., 2020).

Table 2. The result of the thickness of the hydrogel and commercial acne patches

Formulations	Mean (mm)	SD (mm)	CV (%)
CAP 1	0.10	0.0047	4.56
CAP 2	0.10	0.0000	0.00
CAP 3	0.30	0.0047	1.59
F0	0.10	0.0000	0.00
FC1-TTO 1	0.23	0.0000	0.00
FC1-TTO 2	0.21	0.0000	0.00
FC1-TTO 3	0.23	0.0000	0.00
FA1-TTO 1	0.21	0.0047	2.21
FA1-TTO 2	0.29	0.0000	0.00
FA1-TTO 3	0.24	0.0047	1.99

3.2 Functional group of the hydrogel patch

The functional groups of TTO, as well as the hydrogel before (FC1 and FA1) and after TTO loading (FC1-TTO and FA1-TTO), were analyzed using FTIR-ATR spectroscopy, and the spectra are presented in Figure 3. Peaks appearing at wavenumbers 2959-2878 cm^{-1} and

1442-1373 cm^{-1} are associated with C-H stretching, as also reported by Kuptsov and Zhizhin (1998). Additionally, as observed by Hu et al. (2023), these peaks are characteristic components of TTO, such as terpinen-4-ol.

The FTIR analysis of sugar palm starch–chitosan hydrogel before the addition of TTO revealed characteristic peaks at 2884 cm^{-1}, attributed to C-H stretching vibration, 1647 cm^{-1} due to C=O stretching (amide I), and 1413 cm^{-1} corresponding to N-H bending (amide II). These peaks indicate an interaction between the hydroxyl groups of starch and the amine groups of chitosan. Additionally, the sugar palm starch–alginate hydrogel before the addition of TTO exhibited characteristic peaks at 1564 cm^{-1}, attributed to asymmetric C=O stretching, and 1410 cm^{-1}, associated with symmetric C=O stretching (Jiang et al., 2021; Manzanelli et al., 2023).

The FTIR spectra of hydrogels containing TTO showed main peaks at 1408-1420 cm^{-1} and 1333-1334 cm^{-1}. Several characteristic absorption peaks of pure TTO disappeared in the hydrogel form, indicating complete encapsulation of TTO within the hydrogel matrix. These observations aligned with a previous study by Jiang et al. (2021), which reported that the aromatic rings and carbonyl groups of TTO were entirely encapsulated within the hydrogel matrix.

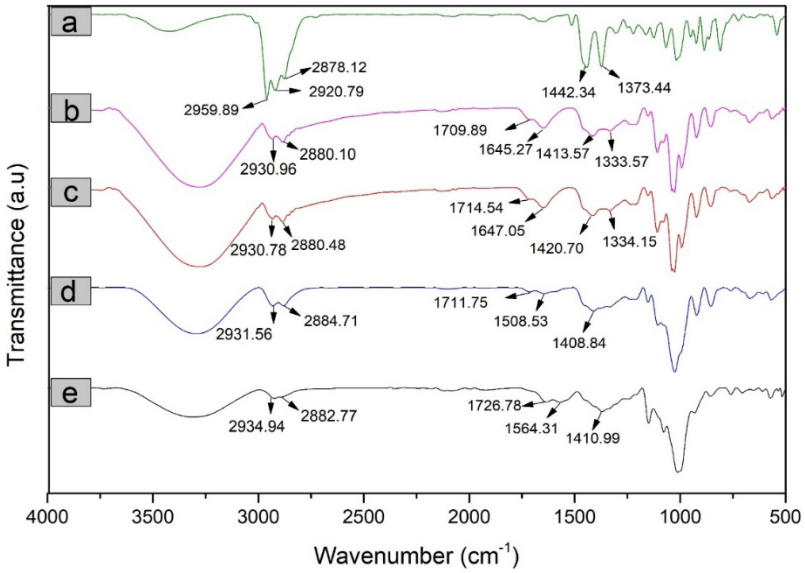

Figure 3. FTIR spectra of TTO (a), FC1-TTO (b), FC1 (c), FA1-TTO (d), FA1 (e)

3.3 Swelling ratio of the hydrogel patch

The swelling ratios of hydrogels loaded with TTO are presented in Figure 4. It was observed that swelling increased over time, with values reaching 197-210% for FC1-TTO and 132-145% for FA1-TTO after 6 h. These results indicate that the type of reinforcing agent had a significant effect on the swelling ratio of the hydrogel ($p<0.05$). This difference can be attributed to the bonding strength with sugar palm starch-alginate hydrogel exhibiting weaker and less flexible bonds. In contrast, the incorporation of TTO at varying concentrations did not significantly affect the swelling ratio ($p>0.05$), based on one-way

ANOVA statistical analysis. According to a literature review conducted by Feng et al. (2023), the swelling ratios of hydrogels for biomedical applications in drug delivery typically exhibited swelling ratios greater than 150%.

However, in this study, commercial acne patches were not included in the swelling ratio analysis due to their distinct formulation compared to hydrogel acne patches developed in this research. Moreover, preliminary observations confirmed that they exhibited no swelling under the same test conditions. These products typically consist of hydrocolloid gels applied onto a flexible polyurethane film, forming a double-layer structure in which the outer layer is water-impermeable (Kuo et al., 2021; Qothrunnadaa & Hasanah, 2021). This study highlights the key advantages of hydrogel-based patches as a promising acne patch-forming material due to their swelling behavior. Based on the swelling data, the FA1-TTO3 and FC1-TTO3 hydrogels were selected for subsequent morphological, thermal, and mechanical analyses.

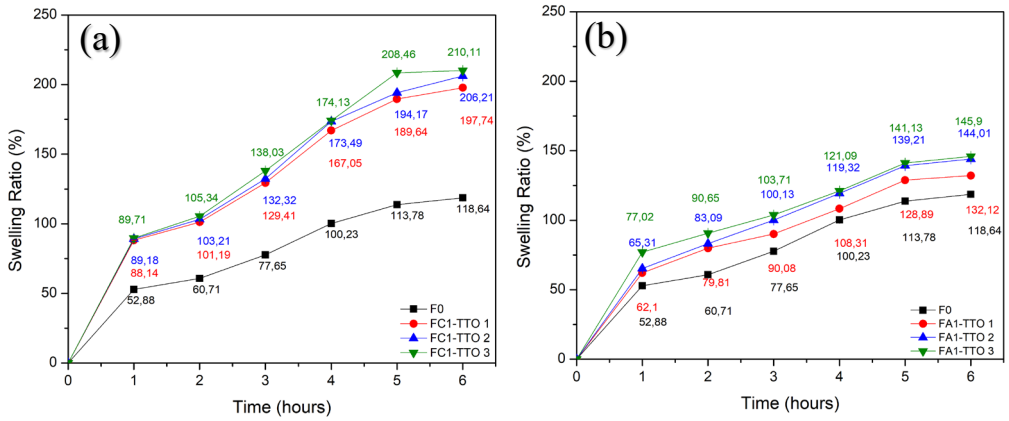

Figure 4. Swelling behaviour of FC1-TTO (a) and FA1-TTO (b) in PBS pH 7.4 at 37°C

3.4 Morphological image of the hydrogel patch

The morphology of the TTO-loaded hydrogels was observed using SEM under 1000x magnification, as shown in Figure 5. The SEM images of the hydrogels before (FC1 and FA1) and after TTO loading (FC1-TTO3 and FA1-TTO3) provide a clear comparison of structural changes. Hydrogels containing TTO showed larger and more irregularly shaped pores compared to hydrogels without TTO, which had small and uniformly shaped pores. This observation indicated that incorporating TTO into the hydrogel alters its internal structure, resulting in increased pore size, irregular pore patterns, and potential agglomeration of TTO particles within the hydrogel surface.

As studied by Wróblewska et al. (2021), the phenomenon arises from the combined effect and interaction between the TTO and the hydrogel matrix formulation. These interactions can lead to the formation of microstructures within the hydrogel matrix. It was also observed that sugar palm starch-chitosan hydrogel loaded with TTO showed a smoother surface compared to sugar palm starch-alginate hydrogel. This phenomenon may be attributed to the reactive amino groups of chitosan, which can interact with the oil, enhancing its dispersion and stabilization within the hydrogel matrix (Sánchez-González et al., 2010). Because hydrophobic oil molecules have a non-polar character, they tend to coagulate and create aggregates when they do not mix well with other substances.

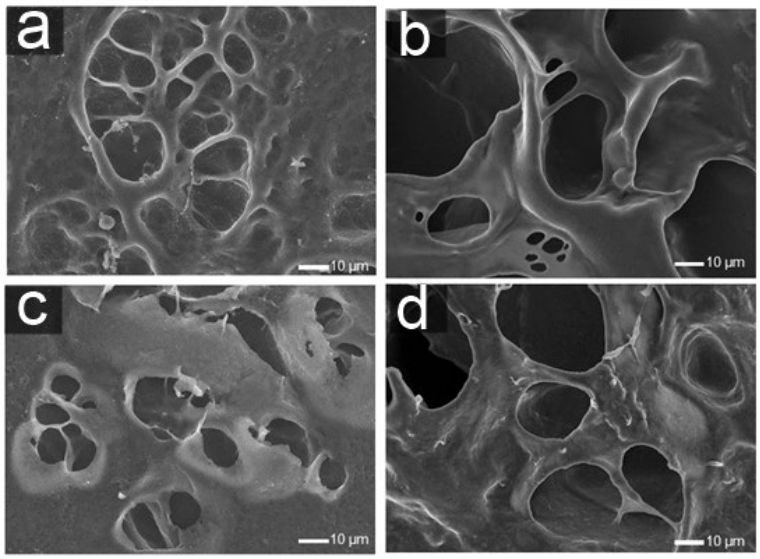

Figure 5. Morphology images of FC1 (a), FC1-TTO3 (b), FA1 (c), and FA1-TTO3 (d)

3.5 Thermal properties of the hydrogel patch

The effect of TTO incorporation on the thermal behavior and phase transitions of the F0, FC1-TTO3 and FA1-TTO3 measured using DSC, with the results presented in Figure 6. The hydrogel without TTO (F0) exhibited a melting temperature (Tm) of 120.4°C. In contrast, hydrogels containing TTO showed an increase in Tm, reaching 132.9°C for the FC1-TTO3 hydrogel and 134.0°C for the FA1-TTO3. This shift in Tm is likely due to interactions between TTO and the polymer matrix, the strength of which depends on the intermolecular forces involved (Morais et al., 2020). As studied by Sathiyaseelan et al. (2023), the combination of chitosan and alginate polymers improves thermal stability when combined with TTO.

The main component of TTO, which is terpinene-4-ol, has a hydroxyl (–OH) group that can form hydrogen bonds with the hydroxyl (-OH) and amino ($–NH_2$) groups in chitosan, resulting in stronger intermolecular interactions (Mielczarek et al., 2023). Although, the carboxylate ($–COO^-$) group in alginate can also form a hydrogen bond with the hydroxyl (–OH) groups in TTO, and these bonds are generally stronger than those in chitosan due to the higher electronegativity of oxygen compared to nitrogen, the melting temperature (Tm) of chitosan-based hydrogels was observed to be higher. This suggests that factors other than hydrogen bond strength, such as polymer structure or interactions, may influence thermal behavior.

That phenomenon is likely related to the semi-crystalline characteristics of chitosan and its abundant interaction sites, which enable the formation of multiple hydrogen bonds that cumulatively strengthen the hydrogel network (Tan et al., 2020; Román-Doval et al., 2023). As a result, more thermal energy is required to disrupt the structure, leading to an elevated Tm. As reported by Jiang et al. (2021) that TTO enhances the strength of the hydrogel network and thermal stability, contributing to higher melting temperatures. In the context of a hydrogel for acne patch application, Tm is crucial for determining its application and performance. Tm indicates the stability of the hydrogel at different temperatures. The

hydrogel patch must remain stable at body temperature (around 37-40°C) during use, which is especially provided in the application of the skin (Fu et al., 2020), and under varying environmental conditions. A low Tm could cause the patch to lose its shape or effectiveness, while a high Tm ensures the patch remains intact and stable under varying environmental conditions (Xin & Lyu, 2023). Since direct comparison with commercial acne patches was not conducted, we provide reference data from polyurethane-based patches for biomedical applications, which have reported Tm range of 119-126°C (Wilson et al., 2019). The Tm observed in this aligns with this range, indicating consistency with prior findings.

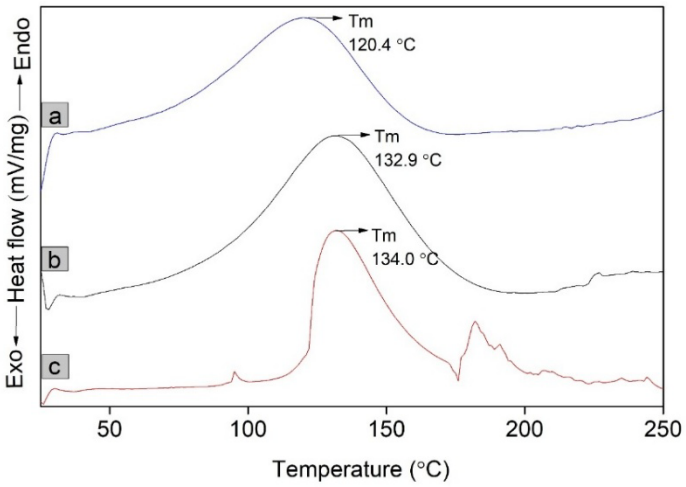

Figure 6. DSC thermogram of F0 (a), FC1-TTO3 (b), and FA1-TTO3 (c)

3.6 Mechanical properties of the hydrogel patch

The mechanical properties of the hydrogel patch loaded with TTO are presented in Table 3, including tensile strength and elongation. Among the formulations, the FC1-TTO3 exhibited lower tensile strength (0.73±0.25 MPa) but greater flexibility, as evidenced by its higher elongation at break value (51.08±1.83%), compared to the elongation value of FA1-TTO3, which was 43.81±16.50%, but showed higher tensile strength (2.15±0.32 MPa). This phenomenon arises because the nitrogen in amino functional group ($–NH_2$) in chitosan has a lower electronegativity compared to the oxygen in carboxylate functional group ($–COO^-$) in alginate, resulting in weaker hydrogen bond interactions that enable greater water retention, forming a less rigid and more flexible network, which allows it to stretch further before breaking.

Table 3. Mechanical properties of the hydrogel patch

Formulation	Mechanical Parameters	
	Tensile Strength (MPa)*	Elongation (%)*
F0	0.07±0.06	21.68±8.00
FC1-TTO3	0.73±0.25	51.08±1.83
FA1-TTO3	2.15±0.32	43.81±16.50

*Values are presented as mean±SD (n = 3).

Statistical analysis using one-way ANOVA confirmed that FA1-TTO3 exhibited significantly higher tensile strength compared to FC1-TTO3 ($p<0.05$). However, no statistically significant difference was observed in elongation between the two groups ($p>0.05$). Although FA1-TTO3 has higher tensile strength, it showed considerable variability in elongation value, as indicated by its high standard deviation (16%). This variability may limit its reliability for applications which require consistent mechanical performance.

The tensile strength values obtained in this study align within the range reported in a previous study by Simões et al. (2020), which range from 1.04-3.83 MPa, and the elongation values obtained in this study exhibit greater elasticity compared to elongation values reported by Khan et al. (2024), which range from 38.67-42.33%. Since a direct comparison with commercial acne patches was not conducted, we provide reference data from polyurethane-based patches used in biomedical applications, which exhibit higher mechanical properties, with tensile strength ranging from 2.2-5.6 MPa and elongation at break ranging from 25.2-64.1% (Gultekin et al., 2009).

3.7 Encapsulation efficiency of hydrogel patch

Encapsulation efficiency is a parameter for evaluating the ability of hydrogels to effectively retain and release active compounds. In this study, the encapsulation efficiencies of FC1-TTO3 and FA1-TTO3 hydrogels were assessed at varying concentrations of TTO. As presented in Table 4, both hydrogels exhibited the highest encapsulation efficiency at a TTO concentration of 100 µg/mL, indicating their optimal capacity to encapsulate TTO at this concentration.

Statistical analysis using one-way ANOVA showed no significant differences in encapsulation efficiency between FA1-TTO3 and FC1-TTO3 across all tested TTO concentrations ($p>0.05$), indicating that both matrix systems were equally effective in encapsulating TTO. Nevertheless, the encapsulation efficiency in FC1-TTO was slightly higher than in FA-TTO. The result was further supported by morphological analysis, which showed that FC1-TTO has a larger pore size than FA1-TTO. The presence of a larger or more porous network enhanced the interaction and distribution of TTO within the hydrogel matrix, leading to increased encapsulation efficiency.

Furthermore, Sánchez-González et al. (2010) reported that chitosan acts as an effective polymer matrix for encapsulating TTO. This arises from the positively charged amino groups in chitosan, which interact electrostatically with the negatively charged phenolic hydroxyl groups in TTO. These electrostatic interactions form strong bonds between chitosan and TTO, enhancing TTO adsorption at the oil-water interface and stabilizing it within the hydrogel matrix.

Table 4. Encapsulation efficiency results of the hydrogel patches

Formulation	Encapsulation Efficiency (%)		
	TTO Loaded (µg/mL)*		
	50	70	100
FC1-TTO	94.25±0.16%	95.52±0.14%	95.98±0.24%
FA1-TTO	95.80±0.07%	95.45±0.22%	95.49±0.35%

*Values are presented as mean±SD (n = 3).

3.8 *In vitro* release of TTO from the hydrogel patch

In vitro testing assesses the physicochemical stability of active compounds and quantitatively measures the release kinetics from the polymer matrix under controlled conditions. This test was conducted based on the principle of a dissolution test, which involves the release of an active substance into a release medium. In this study, ethanol 96% was used as the release medium for TTO. The release profiles of TTO from the FC1-TTO hydrogel and FA1-TTO hydrogel are presented in Figure 7, demonstrating that as the concentration of TTO added to the hydrogel formulation increased, the amount of TTO released also increased.

Among all the tested concentrations, the highest release rate was observed at 100 µg/mL of TTO, compared to 50 and 70 µg/mL. A significant increase in the release of the active substance occurred during the first 1 to 4 h, as confirmed by one-way ANOVA analysis ($p<0.05$). This was followed by a slower release rate between 5 and 6 h, after which the release approached equilibrium. After 6 h, the highest cumulative release of TTO from the sugar palm starch-based hydrogel was observed in FC1-TTO 3, reaching 64.14%, whereas FA1-TTO 3 reached 85.08%. That suggests that the type of reinforcing agent significantly influences TTO release in the hydrogel, as confirmed by one-way ANOVA statistical analysis ($p<0.05$).

Although FA1-TTO exhibited a higher release rate, the sugar palm starch-alginate hydrogel tended to degrade more quickly in the release medium. This degradation compromised the reliability of the data, as the damaged matrix could no longer effectively encapsulate the active compound, indicating that the hydrogel matrix was less capable to maintaining its structural integrity. For acne patch applications, the release needs to be stable over 6-8 h to avoid a burst release, which was evident in FA1-TTO. Therefore, FC1-TTO demonstrated the most appropriate release profile. This behaviour was likely attributable to the higher hydrophobicity of alginate compared to chitosan, affecting its interaction with the lipophilic tea tree oil (TTO) (Sathiyaseelan et al., 2023).

The TTO release values observed in this study aligned with the ranges reported by previous research. For instance, Hu et al. (2023) documented a TTO release of 41.50% from chitosan-based hydrogels, while Yeh et al. (2011) reported approximately 90.00% release from alginate hydrogels. These differences highlight the impact of the hydrogel polymer type on the TTO release behavior.

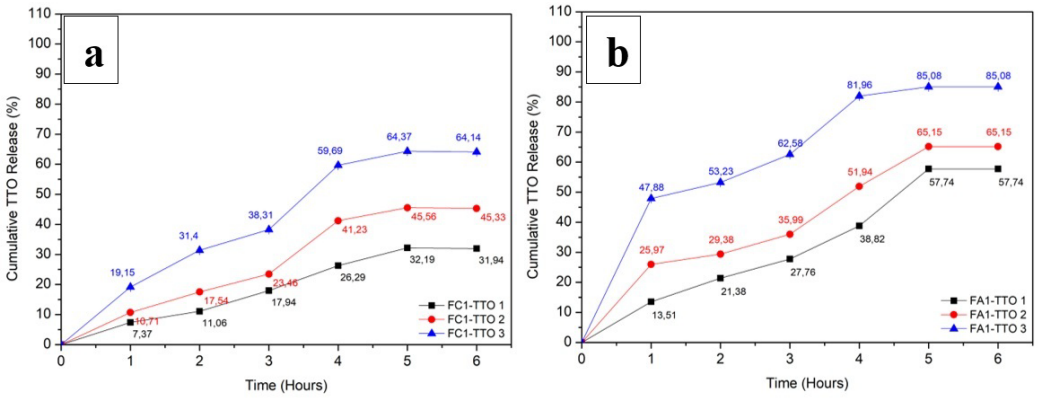

Figure 7. *In vitro* release graphics of FC1-TTO (a) and FA1-TTO (b) in PBS pH 7.4 at 37°C

3.9 Antibacterial activity assay of hydrogel patch

The inhibition zone for sugar palm starch-based hydrogel-loaded TTO exhibited good antibacterial activity against Gram-positive strains *C. acnes, S. aureus,* and *S. epidermidis,* which are known as acne-causing bacteria. The results indicated that TTO inhibited cellular growth and showed a dose-dependent inhibitory action on the bacterial cells. As the concentration of TTO increased, the zone of inhibition also increased. The detailed inhibition zone measurements for each formulation (FC1-TTO 1-3 and FA1-TTO 1-3) are presented in Table 5. As studied by Rehman et al. (2024), higher concentrations of TTO can result in a wider and more even distribution of TTO on the surface of bacteria or in the surrounding environment, potentially leading to more production of reactive oxygen species (ROS) at active sites, which interact with bacterial cell structures and damage bacterial membranes.

The bacteria inhibition zone for TTO in this study related to the literature review by Nascimento et al. (2023). The inhibition zones for TTO in many research studies using TTO were 20.85 mm for *C. acnes*, 16.57-19.20 mm for *S. aureus*, and 19.20-21.7 mm for *S. epidermidis* (Nascimento et al., 2023). For comparison, vancomycin used as a positive control (control (+)) in this study formed clear zones of 18.50 mm for *C. acnes*, 17.40 mm for *S. aureus*, and 18.00 mm for *S. epidermidis*. According to Clinical and Laboratory Standards Institute (CLSI) standards, these values fall into the sensitive category (≥17 mm) (Patel et al., 2015), confirming the effectiveness of vancomycin in inhibiting acne-causing bacteria. Meanwhile, the hydrogel without active ingredients, as a negative control (control (-)) showed no inhibition.

In this study, we also evaluated the impact of washing hydrogels with water, specifically to remove citric acid, on their antibacterial activity. Citric acid, used as a cross-linking agent, was found to have a minimal effect on the antibacterial properties of the hydrogels after washing. Both washed and unwashed hydrogels exhibited consistent antibacterial activity, suggesting that residual citric acid post-washing was minimal or not a key factor in bacterial inhibition. These findings highlight the stability and effectiveness of the hydrogels even after washing. To visualize the antibacterial activity, Figure 8 presents petri dish images showing inhibition zones for each formulation tested against *C. acnes, S. aureus,* and *S. epidermidis*. The inhibition zones appear as clear zones around the hydrogel samples, indicating bacterial growth suppression.

Table 5. Zone of inhibition of the TTO-loaded hydrogel patches and control

Formulation	Inhibition Zone of Bacteria (mm)*		
	C. acnes	***S. aureus***	***S. epidermidis***
Control (-)	0.00±0.00	0.00±0.00	0.00±0.00
Control (+)	18.50±0.00	17.40±0.00	18.00±0.00
FC1-TTO 1	10.00±0.00	12.00±0.80	12.00±1.20
FC1-TTO 2	13.00±1.40	14.00±1.60	15.00±0.00
FC1-TTO 3	16.00±0.80	17.00±1.20	18.00±1.20
FA1-TTO 1	10.00±0.00	10.00±0.40	10.00±0.40
FA1-TTO 2	11.00±0.40	11.00±0.80	14.00±1.60
FA1-TTO 3	14.00±0.90	13.00±1.70	18.00±1.40

*Values are presented as mean±SD (n = 3).

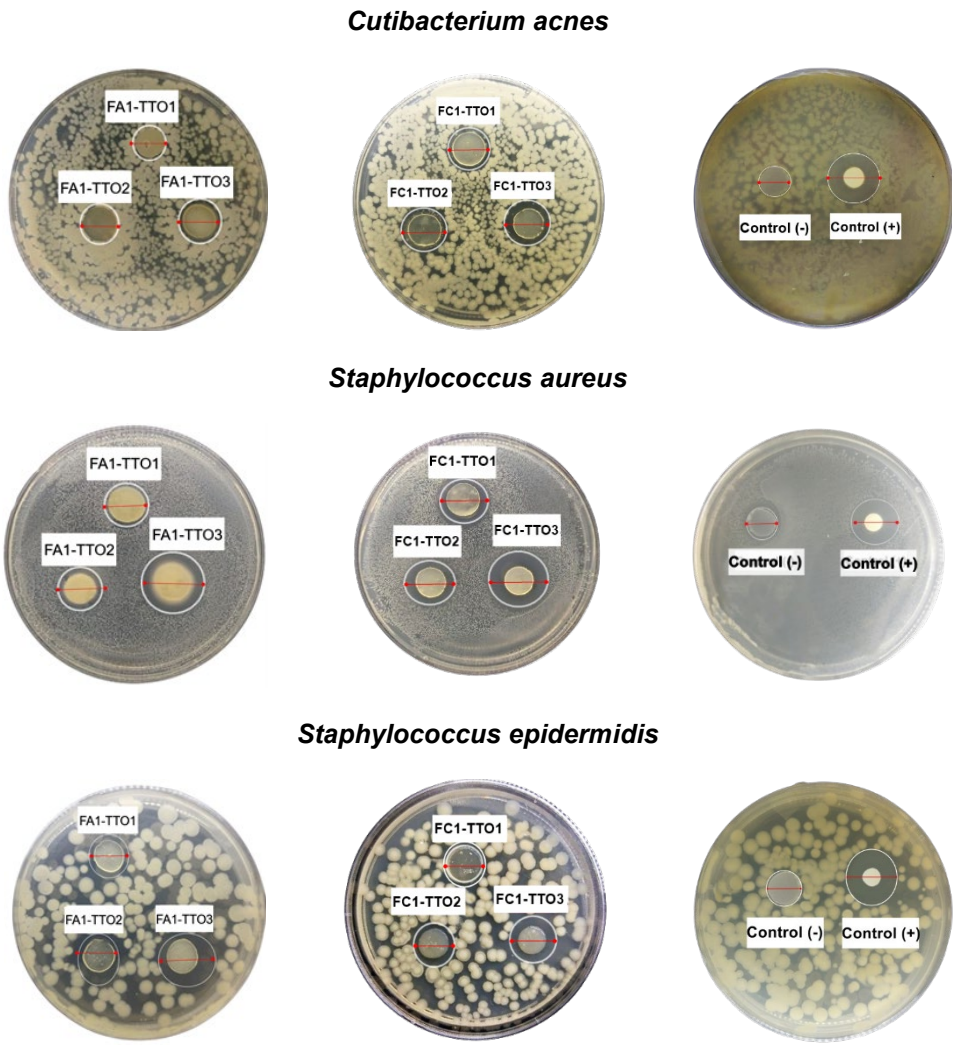

Figure 8. Antibacterial activity of the TTO-loaded hydrogel patches

3.10 Stability test of the hydrogel patch

The physical stability of hydrogel patches was assessed over 7 days under accelerated storage conditions at 4°C, 25°C, and 40°C, and evaluated based on changes in color and weight. All formulations maintained their initial color, which was translucent white for FC1-TTO and yellowish-brown for FA1-TTO, without any visible degradation or discoloration. The weights of hydrogel patches on day 7 changed compared to day 0, measured as a percentage of weight change (weight change %), which are presented in Table 6.

Hydrogel patches at low temperatures (4°C) exhibited weight gain, ranging from 72.45-80.00% for FC1-TTO and 72.86-76.15% for FA1-TTO. In contrast, at room temperature (25°C), the patches exhibited good physical stability, as demonstrated by minimal weight fluctuations, ranging from 7.14-7.65% for FC1-TTO and 7.14-8.57% for

FA1-TTO. However, at high temperatures (40°C), the hydrogels exhibited weight loss ranging from 10.00-14.35% for FC1-TTO and 10.00-12.38% for FA1-TTO.

Overall, these results indicate that the hydrogel patches demonstrated optimal stability at room temperature, swelling at low temperatures due to moisture uptake, and weight loss at elevated temperatures likely caused by evaporation and partial polymer degradation. These findings illustrate the temperature-dependent behavior of the hydrogels as indicated by Kuth and Boccaccini (2024). These observations also highlight the need for further optimization of the formulations to enhance their performance under extreme conditions.

Table 6. Stability test result of the hydrogel patches

Sample Code	Temp (°C)	Weight (g)*		Weight Change (%)*
		Day 0	Day 7	
FC1-TTO1	4	0.0311±0.00	0.0537±0.00	72.45±0.00
	25	0.0280±0.00	0.0301±0.00	7.38±0.00
	40	0.0271±0.00	0.0239±0.00	-11.76±0.00
FC1-TTO2	4	0.0302±0.00	0.0544±0.00	80.00±0.00
	25	0.0273±0.00	0.0294±0.00	7.65±0.00
	40	0.0300±0.00	0.0270±0.00	-10.00±0.00
FC1-TTO3	4	0.0291±0.00	0.0518±0.00	77.89±0.00
	25	0.0285±0.00	0.0305±0.00	7.14±0.00
	40	0.0312±0.00	0.0267±0.00	-14.35±0.00
FA1-TTO1	4	0.0367±0.00	0.0646±0.00	76.15±0.00
	25	0.0388±0.00	0.0416±0.00	7.14±0.00
	40	0.0419±0.00	0.0377±0.00	-10.00±0.00
FA1-TTO2	4	0.0440±0.00	0.0766±0.00	74.12±0.00
	25	0.0451±0.00	0.0490±0.00	8.57±0.00
	40	0.0416±0.00	0.0364±0.00	-12.38±0.00
FA1-TTO3	4	0.0388±0.00	0.0671±0.00	72.86±0.00
	25	0.0419±0.00	0.0452±0.00	7.88±0.00
	40	0.0392±0.00	0.0344±0.00	-12.22±0.00

*Values are presented as mean±SD (n = 3).

4. Conclusions

The results show that both sugar palm starch-chitosan and sugar palm starch-alginate hydrogels with 50-100 µg/mL of TTO are effective against *C. acnes, S. aureus,* and *S. epidermidis*, the key acne-causing bacteria. The sugar palm starch-chitosan hydrogel has a slightly higher encapsulation efficiency (95.98±0.24%) compared to the sugar palm starch-alginate hydrogel (95.49±0.35%). However, the TTO release was slower from the starch-chitosan hydrogel (64.14% over 6 hours) compared to the sugar palm starch-alginate hydrogel (85.08%). The results indicate that hydrogels with higher concentrations

of TTO exhibit stronger bacterial inhibition. The hydrogel patches remained stable at room temperature but gained weight at low temperatures and lost weight at high temperatures.

5. Acknowledgements

The authors acknowledge the facilities and scientific and technical support from Advanced Characterization Laboratories Serpong, National Research and Innovation Agency (BRIN) through E-Layanan Sains, Badan Riset dan Inovasi Nasional.

6. Authors' Contributions

Tazkia Qonita Zahra, Witta Kartika Restu: Conceptualization, Tazkia Qonita Zahra: Writing -original draft preparation, Tazkia Qonita Zahra, Witta Kartika Restu, Noverrra M. Nizardo: Writing, review, and editing, Witta Kartika Restu, Noverrra M. Nizardo: Supervision, Witta Kartika Restu: Funding acquisition.

ORCID
Tazkia Qonita Zahra https://orcid.org/0000-0002-4618-1332
Noverra M. Nizardo https://orcid.org/0000-0002-7022-2210
Witta Kartika Restu https://orcid.org/0000-0002-7536-3610

7. Conflicts of Interest

The authors have declared that they have no conflicts of interests.

References

Adawiyah, D. R., Sasaki, T., & Kohyama, K. (2013). Characterization of arenga starch in comparison with sago starch. *Carbohydrate Polymers*, *92*(2), 2306-2313. https://doi.org/10.1016/j.carbpol.2012.12.014

Aranaz, I., Alcántara, A. R., Civera, M. C., Arias, C., Elorza, B., Caballero, A. H., & Acosta, N. (2021). Chitosan: An overview of its properties and applications. *Polymers*, *13*(19), Article 3256. https://doi.org/10.3390/polym13193256

Arpa, M. D., Okur, N. Ü., Gök, M. K., Özgümüş, S., & Cevher, E. (2023). Chitosan-based buccal mucoadhesive patches to enhance the systemic bioavailability of tizanidine. *International Journal of Pharmaceutics*, *642*, Article 123168. https://doi.org/10.1016/j.ijpharm.2023.123168

Beheshti-Mall, L., Shafaroodi, H., Jafariazar, Z., & Afshar, M. (2018). A novel hydrogel-thickened microemulsion of dapsone for acne treatment: Development, characterization, physicochemical stability and ex vivo permeation studies. *Marmara Pharmaceutical Journal*, *22*(2), 267-276. https://doi.org/10.12991/mpj.2018.64

Berradi, A., Aziz, F., Achaby, M. El, Ouazzani, N., & Mandi, L. (2023). A comprehensive review of polysaccharide-based hydrogels as promising biomaterials. *Polymers*, *15*(13), Article 2908. https://doi.org/10.3390/polym15132908

Bisht, A., Hemrajani, C., Rathore, C., Dhiman, T., Rolta, R., Upadhyay, N., Nidhi, P., Gupta, G., Dua, K., Chellappan, D. K., Dev, K., Sourirajan, A., Chakraborty, A., Aljabali, A. A. A., Bakshi, H. A., Negi, P., & Tambuwala, M. M. (2022). Hydrogel composite containing azelaic acid and tea tree essential oil as a therapeutic strategy for

Propionibacterium and testosterone-induced acne. *Drug Delivery and Translational Research*, *12*(10), 2501-2517. https://doi.org/10.1007/s13346-021-01092-4

Feng, W., & Wang, Z. (2023). Tailoring the swelling-shrinkable behavior of hydrogels for biomedical applications. *Advanced Science*, *10*(28), Article 2303326. https://doi.org/10.1002/advs.202303326

Fu, G. Q., Zhang, S. C., Chen, G. G., Hao, X., Bian, J., & Peng, F. (2020). Xylan-based hydrogels for potential skin care application. *International Journal of Biological Macromolecules*, *158*, 244-250. https://doi.org/10.1016/j.ijbiomac.2020.04.235

Greay, S. J., Ireland, D. J., Kissick, H. T., Levy, A., Beilharz, M. W., Riley, T. V., & Carson, C. F. (2010). Induction of necrosis and cell cycle arrest in murine cancer cell lines by *Melaleuca alternifolia* (tea tree) oil and terpinen-4-ol. *Cancer Chemotherapy and Pharmacology*, *65*(5), 877-888. https://doi.org/10.1007/s00280-009-1093-7

Gultekin, G., Atalay-Oral, C., Erkal, S., Sahin, F., Karastova, D., Tantekin-Ersolmaz, S. B., & Guner, F. S. (2009). Fatty acid-based polyurethane films for wound dressing applications. *Journal of Materials Science: Materials in Medicine*, *20*(1), 421-431. https://doi.org/10.1007/s10856-008-3572-5

Hu, K., Jia, E., Zhang, Q., Zheng, W., Sun, R., Qian, M., Tan, Y., & Hu, W. (2023). Injectable carboxymethyl chitosan-genipin hydrogels encapsulating tea tree oil for wound healing. *Carbohydrate Polymers*, *301*(Part B), Article 120348. https://doi.org/10.1016/j.carbpol.2022.120348

Jiang, S., Zhao, T., Wei, Y., Cao, Z., Xu, Y., Wei, J., Xu, F., Wang, H., & Shao, X. (2021). Preparation and characterization of tea tree oil/ hydroxypropyl-β-cyclodextrin inclusion complex and its application to control brown rot in peach fruit. *Food Hydrocolloids*, *121*, Article 107037. https://doi.org/10.1016/j.foodhyd.2021.107037

Jumaidin, R., Sapuan, S. M., Jawaid, M., Ishak, M. R., & Sahari, J. (2016). Characteristics of thermoplastic sugar palm starch/agar blend: Thermal, tensile, and physical properties. *International Journal of Biological Macromolecules*, *89*, 575-581. https://doi.org/10.1016/j.ijbiomac.2016.05.028

Khan, N., Pawar, A. P., Patil, S., Patil, R., Patil, V., Patil, N., Dalvi, S. R., Kshirsagar, S. V, & Kale, M. (2024). Formulation and evaluation of polyherbal anti-acne patch. *MGM Journal of Medical Sciences*, *11*(2), 34-41. https://doi.org/10.4103/mgmj.mgmj_137_24

Kuo, C.-W., Chiu, Y.-F., Wu, M.-H., Li, M.-H., Wu, C.-N., Chen, W.-S., & Huang, C.-H. (2021). Gelatin/chitosan bilayer patches loaded with cortex *Phellodendron amurense/Centella asiatica* extracts for anti-acne application. *Polymers*, *13*(4), Article 579. https://doi.org/10.3390/polym13040579

Kuptsov, A. H., & Zhizhin, G. N. (1998). *Handbook of fourier transform raman and infrared spectra of polymers*. Elsevier.

Kuth, S., & Boccaccini, A. R. (2024). Enzymatic in situ crosslinking can improve hydrogel stability while maintaining matrix stiffness. *ChemistrySelect*, *9*(33), Article e202401700. https://doi.org/10.1002/slct.202401700

Manzanelli, F. A., Ravetti, S., Brignone, S. G., Garro, A. G., Martínez, S. R., Vallejo, M. G., & Palma, S. D. (2023). Enhancing the functional properties of tea tree oil: In vitro antimicrobial activity and microencapsulation strategy. *Pharmaceutics*, *15*(10), Article 2489. https://doi.org/10.3390/pharmaceutics15102489

Mielczarek, M., Marchewka, J., Kowalski, K., Cieniek, Ł., Sitarz, M., & Moskalewicz, T. (2023). Effect of tea tree oil addition on the microstructure, structure and selected properties of chitosan-based coatings electrophoretically deposited on zirconium alloy substrates. *Applied Surface Science*, *609*, Article 155266. https://doi.org/10.1016/j.apsusc.2022.155266

Morais, F. P., Simões, R. M. S., & Curto, J. M. R. (2020). Biopolymeric delivery systems for cosmetic applications using *Chlorella vulgaris* algae and tea tree essential oil. *Polymers*, *12*(11), Article 2689. https://doi.org/10.3390/polym12112689

Nascimento, T., Gomes, D., Simões, R., & Miguel, M. D. G. (2023). Tea tree oil: Properties and the therapeutic approach to acne—A review. *Antioxidants*, *12*(6), Article 1264. https://doi.org/10.3390/antiox12061264

Parhi, R. (2017). Cross-linked hydrogel for pharmaceutical applications: A review. *Advanced Pharmaceutical Bulletin*, *7*(4), 515-530. https://doi.org/10.15171/apb.2017.064

Patel, J. B., Cockerill, F. R. III, Bradford, P. A., Eliopoulos, G. M., Hindler, J. A., Jenkins, S. G., Lewis, J. S. II, Limbago, B., Miller, L. A., Nicolau, D. P., Powell, M., Swenson, J. M., Traczewski, M. M., Turnidge, J. D., Weinstein, M. P., & Zimmer, B. L. (2015). *M100-S25 Performance standards for antimicrobial susceptibility testing; Twenty-fifth informational supplement.* Clinical and Laboratory Standards Institute.

Qothrunnadaa, T., & Hasanah, A. N. (2021). Patches for acne treatment: An update on the formulation and stability test. *International Journal of Applied Pharmaceutics*, *13*(4), 21-26. https://doi.org/10.22159/IJAP.2021.V13S4.43812

Reddy, N., Reddy, R., & Jiang, Q. (2015). Crosslinking biopolymers for biomedical applications. *Trends in Biotechnology*, *33*(6), 362-369. https://doi.org/10.1016/j.tibtech.2015.03.008

Rehman, S., Ravinayagam, V., Al-Jameel, S. S., Ali, S. M., Alzayer, S. Z., Alfaraj, Z. M., Alboeid, A., Alamri, N., Al Isam, S. H., Dafallae, H., Dhanasekaran, S., Tanimu, G., Khan, F. A., & Jermy, B. R. (2024). Controlling cisplatin release by synergistic action of silver-cisplatin on monodispersed spherical silica for targeted anticancer and antibacterial activities. *Arabian Journal of Chemistry*, *17*(4), Article 105661. https://doi.org/10.1016/j.arabjc.2024.105661

Román-Doval, R., Torres-Arellanes, S. P., Tenorio-Barajas, A. Y., Gómez-Sánchez, A., & Valencia-Lazcano, A. A. (2023). Chitosan: Properties and its application in agriculture in context of molecular weight. *Polymers*, *15*(13), Article 2867. https://doi.org/10.3390/polym15132867

Sánchez-González, L., González-Martínez, C., Chiralt, A., & Cháfer, M. (2010). Physical and antimicrobial properties of chitosan-tea tree essential oil composite films. *Journal of Food Engineering*, *98*(4), 443-452. https://doi.org/10.1016/j.jfoodeng.2010.01.026

Sanyang, M. L., Sapuan, S. M., Jawaid, M., Ishak, M. R., & Sahari, J. (2016). Recent developments in sugar palm (*Arenga pinnata*) based biocomposites and their potential industrial applications: A review. *Renewable and Sustainable Energy Reviews*, *54*, 533-549. https://doi.org/10.1016/j.rser.2015.10.037

Sathiyaseelan, A., Zhang, X., & Wang, M.-H. (2023). Enhancing the antioxidant, antibacterial, and wound healing effects of melaleuca alternifolia oil by microencapsulating it in chitosan-sodium alginate microspheres. *Nutrients*, *15*(6), Article 1319. https://doi.org/10.3390/nu15061319

Simões, B. M., Cagnin, C., Yamashita, F., Olivato, J. B., Garcia, P. S., de Oliveira, S. M., & Grossmann, M. V. E. (2020). Citric acid as crosslinking agent in starch/xanthan gum hydrogels produced by extrusion and thermopressing. *LWT*, *125*, Article 108950. https://doi.org/10.1016/j.lwt.2019.108950

Tan, Q., Kan, Y., Huang, H., Wu, W., & Lu, X. (2020). Probing the molecular interactions of chitosan films in acidic solutions with different salt ions. *Coatings*, *10*(11), Article 1052. https://doi.org/10.3390/coatings10111052

Tomić, S. L., Babić Radić, M. M., Vuković, J. S., Filipović, V. V., Nikodinovic-Runic, J., & Vukomanović, M. (2023). Alginate-based hydrogels and scaffolds for biomedical applications. *Marine Drugs*, *21*(3), Article 177. https://doi.org/10.3390/md21030177

Wilpiszewska, K., Antosik, A. K., & Zdanowicz, M. (2019). The effect of citric acid on physicochemical properties of hydrophilic carboxymethyl starch-based films. *Journal of Polymers and the Environment*, *27*(6), 1379-1387. https://doi.org/10.1007/s10924-019-01436-9

Wilson, A. C., Chou, S.-F., Lozano, R., Chen, J. Y., & Neuenschwander, P. F. (2019). Thermal and physico-mechanical characterizations of thromboresistant polyurethane films. *Bioengineering*, *6*(3), Article 69. https://doi.org/10.3390/bioengineering6030069

Wróblewska, M., Szymańska, E., & Winnicka, K. (2021). The influence of tea tree oil on antifungal activity and pharmaceutical characteristics of pluronic®F-127 gel formulations with Ketoconazole. *International Journal of Molecular Sciences*, *22*(21), Article 11326. https://doi.org/10.3390/ijms222111326

Xin, F., & Lyu, Q. (2023). A review on thermal properties of hydrogels for electronic devices applications. *Gels, 9*(1), Article 7. https://doi.org/10.3390/gels9010007

Yeh, K. W., Chang, C. P., Yamamoto, T., & Dobashi, T. (2011). Release model of alginate microcapsules containing volatile tea-tree oil. *Colloids and Surfaces A: Physicochemical and Engineering Aspects*, *380*(1-3), 152-155. https://doi.org/10.1016/j.colsurfa.2011.02.043

Zhang, S., Chen, J., Yin, X., Wang, X., Qiu, B., Zhu, L., & Lin, Q. (2017). Microencapsulation of tea tree oil by spray-drying with methyl cellulose as the emulsifier and wall material together with chitosan/alginate. *Journal of Applied Polymer Science*, *134*(13), Article 44662. https://doi.org/10.1002/app.44662